Supplemental Information

Collateral Pathways from the Ventromedial

Hypothalamus Mediate Defensive Behaviors

Li Wang, Irene Z. Chen, and Dayu Lin
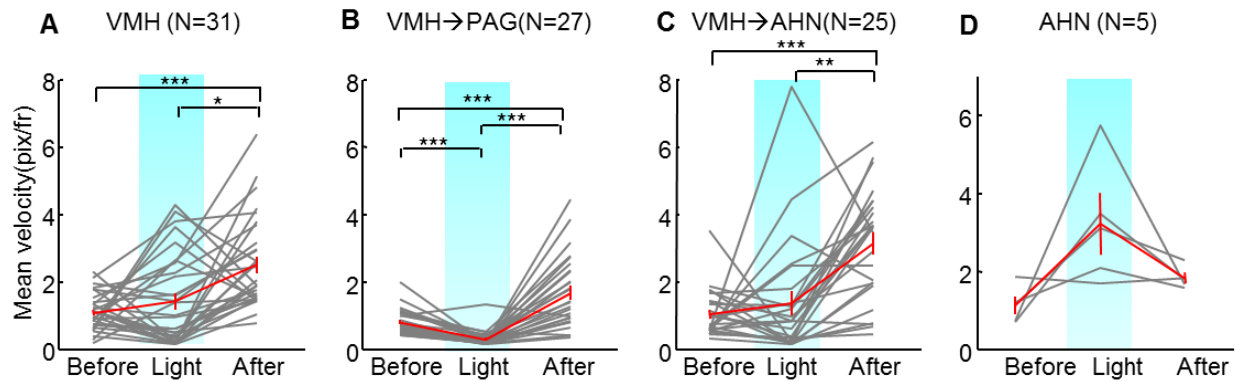
SUPPLEMENTAL FIGURES AND LEGENDS

Figure S1 (related to Figure 2). VMH, VMH→PAG, VMH→AHN and AHN stimulations induced velocity changes in the home cage. Plots show the mean velocity before, during and after VMH (A, N =31), VMH→PAG (B, N =27), VMH→AHN (C, N=25) and AHN (D, N=5) stimulations. Gray lines represent individual animals. Red lines show population averages. Error bars: standard errors. Paired *t*-test with FDR adjustment. *$p < 0.05$, **$p < 0.01$, ***$p < 0.001$.

A Light on   Light on

top view   XY velocity

immobile   run   immobile   run

5 Pix/Fr

B side view

Distance from ground

Z velocity

jump   jump

100 Pix

50 Pix/Fr

10s

C

Immobile

Run

Jump

— Light   — Ann 1   — Comp   — Ann 2

100 s

D

% Immobile

Computer

r = 0.781   Annotator 1

Annotator 2

r = 0.827   Annotator 1

Annotator 2

r = 0.802   Computer

E

Running No.

Computer

r = 0.8501   Annotator 1

Annotator 2

r = 0.864   Annotator 1

Annotator 2

r = 0.944   Computer

F

Jumping No.

Computer

r = 0.9093   Annotator 1

Annotator 2

r = 0.9611   Annotator 1
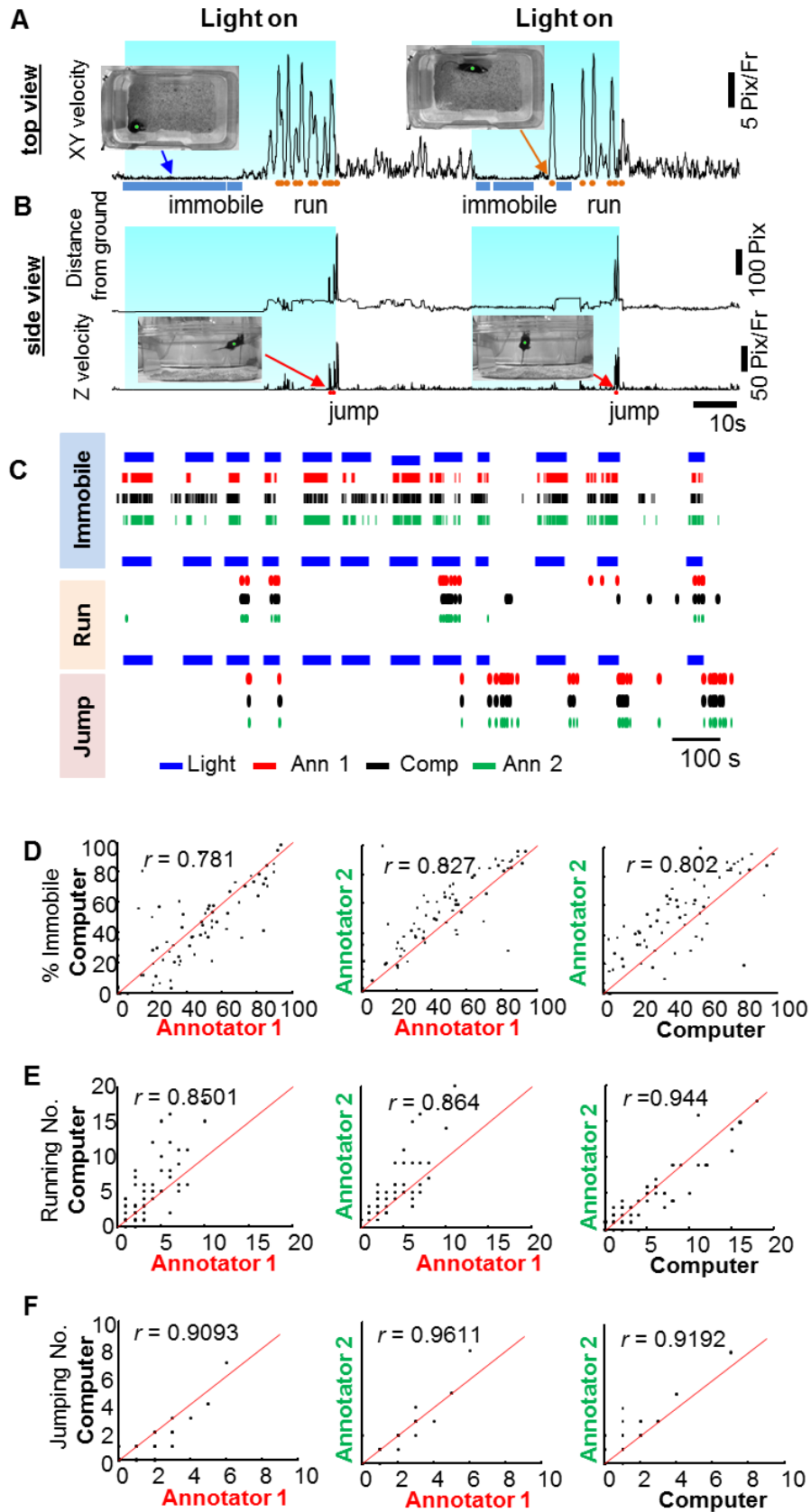
Annotator 2

r = 0.9192   Computer

Figure S2 (related to Figure 2). Comparisons between computer annotations and human annotations. (A) XY-plane velocity based on top view video. Computer annotated immobility period (blue) and running events (orange dots) are indicated. (B) Vertical velocity and distance above the cage floor based on side-view video. Jump events are indicated by red dots. (C) Example raster plots show human- and computer-annotated immobility, running and jumping events. Blue: Light on; red and green: human annotations; black: computer annotation. (D–F) Correlation between human and computer annotations. Each dot represents one light stimulation trial. The correlation coefficient for each plot is shown at the upper left corner.
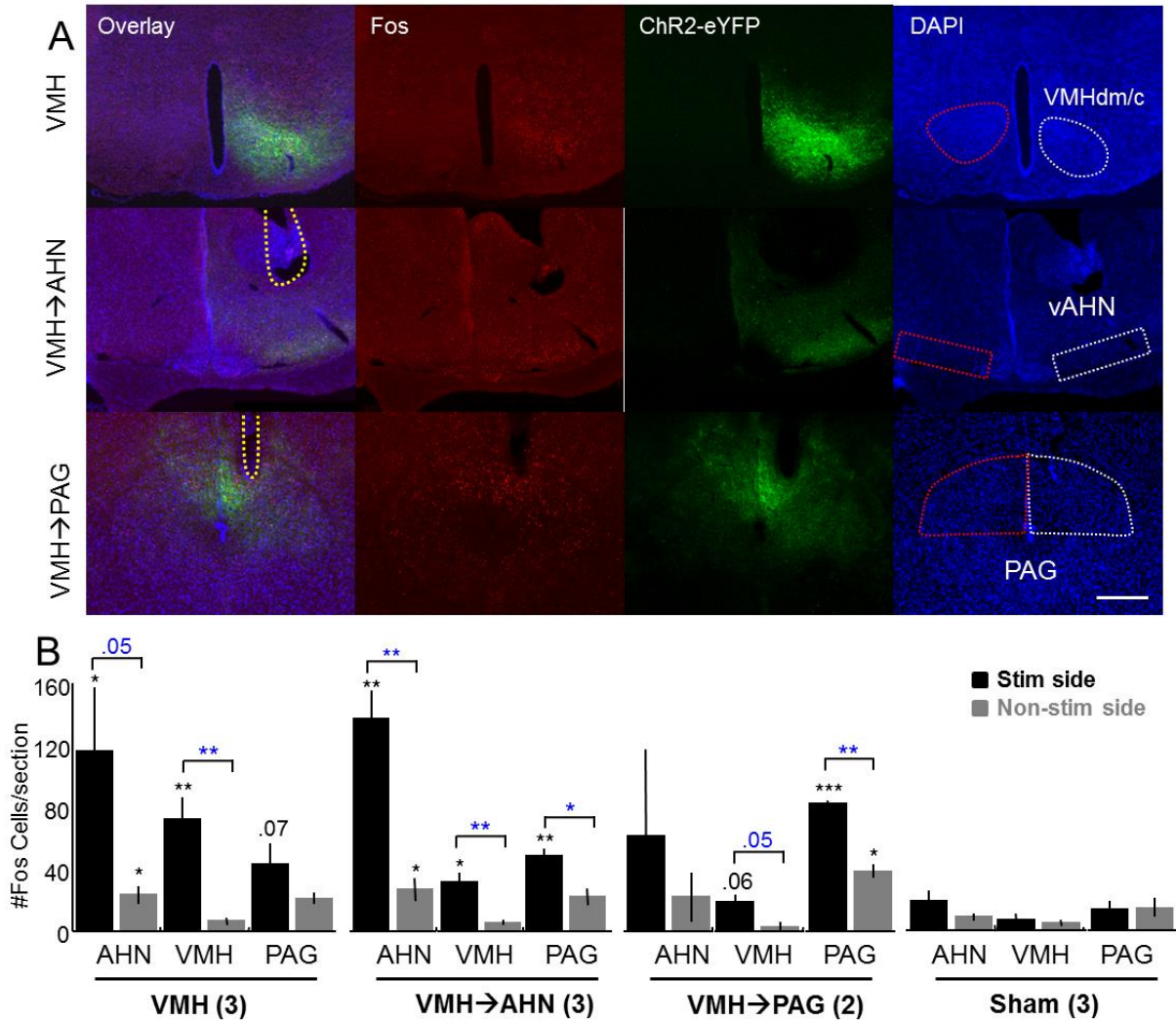
Figure S3 (related to Figure 5): Fos expression induced by light stimulation of the VMHdm/c and its terminals. (A) Representative pictures showing Fos expression (red) at the VMH after VMH stimulation (top panel), at the AHN after VMH→AHN stimulation (middle panel) and at the PAG after VMH→PAG stimulation (bottom panel). Areas of Fos counted are indicated by white (stimulation side) and red (non-stimulation side) dashed lines in DAPI (blue) counterstaining pictures. Green: endogenous ChR2-EYFP. Scale bars: 500 μm. Dashed yellow lines mark optic fiber tracks. (B) Average number of Fos positive cells per section in the AHN, VMH and PAG after VMH, VMH→ AHN, VMH→PAG and sham (with fiber insertion)

stimulations. In general, after stimulation, Fos increased in all three regions bilaterally, more in the stimulation side and less in the non-stimulation side, except the VMH, which showed increase only in the stimulation side. VMH→AHN stimulation induced Fos most strongly in the AHN but also in the VMH and PAG to a lesser extent. Similarly, VMH→PAG stimulation induced Fos most strongly in the PAG but also in the VMH and AHN to a lesser extent. Black bars: stimulation side; Grey bars: non-stimulation side. Two-way ANOVA for each stimulation condition revealed the main factors contributing to the variability in the number of Fos-expressing cells (stimulation side vs. non stimulation, real stimulation vs. sham stimulation and their interaction term). If a significant contributor to the variability is identified ($p < 0.05$), the *t*-test was performed either between the stimulation side and non-stimulation side or between real and sham stimulation groups (side matched). Black * indicates *t*-test result comparing real stimulation and sham stimulation groups. Blue * indicates *t*-test result comparing stimulation side and non-stimulation side. *$p < 0.05$, **$p < 0.01$, ***$p < 0.001$. All p values below 0.1 are indicated. Error bars: standard errors.
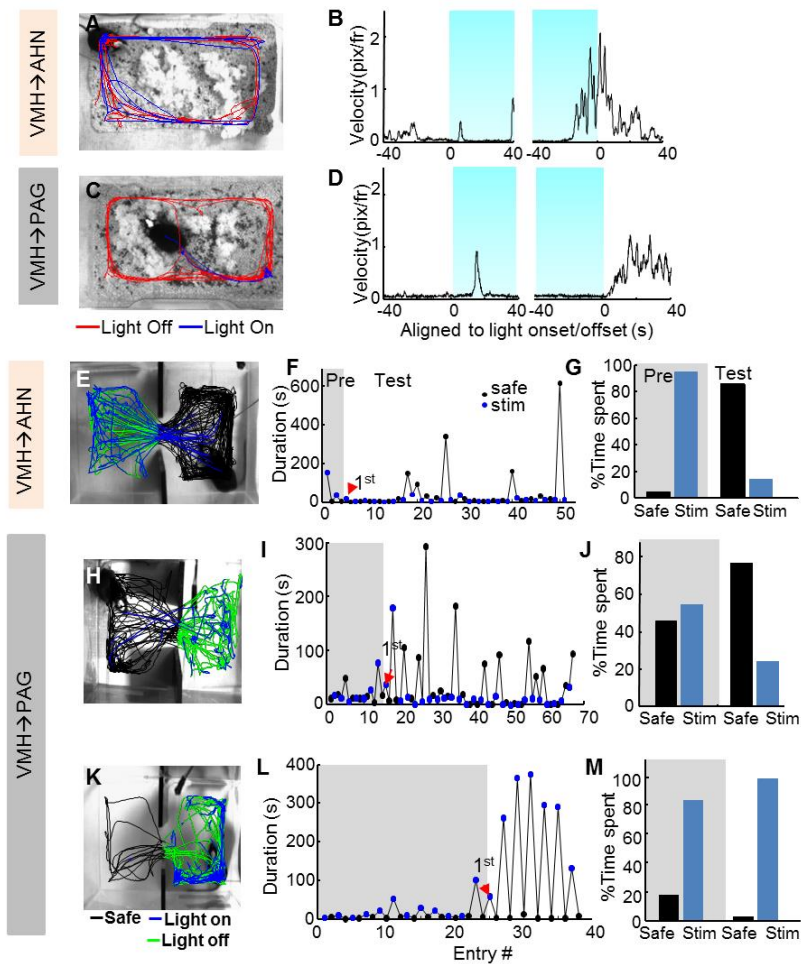
Figure S4 (related to Figure 5). Examples of behavioral changes induced by VMH→AHN or VMH→PAG stimulation in the home cage and real-time place preference test. (A and C) Examples of tracking traces with 20-Hz VMH→AHN (A) and VMH→PAG (C) stimulations in home cage. Blue: light on; red: light off. Each trace contains six stimulation trials. (B and D) The average velocity over time aligned to stimulation onset (left) and stimulation offset (right). Blue shading indicates the light-on period. (E–G) VMH→AHN stimulation caused avoidance of the stimulation chamber. (H–J) VMH→PAG stimulation caused avoidance of the stimulation chamber. (K–M) VMH→PAG stimulation did not elicit avoidance to the stimulation chamber. (E, H, and K) tracking traces. Blue: light on; green: light off in stimulation chamber; black: safe

chamber. (F, I, and L) The time spent in stimulation chamber (blue dots) and safe chamber (black dots) per entry over entry number. Red arrows indicate first entry into the stimulation chamber during test. (G, J, and M) The percentage of time animal spent in each chamber during pretest (gray shade) and test.
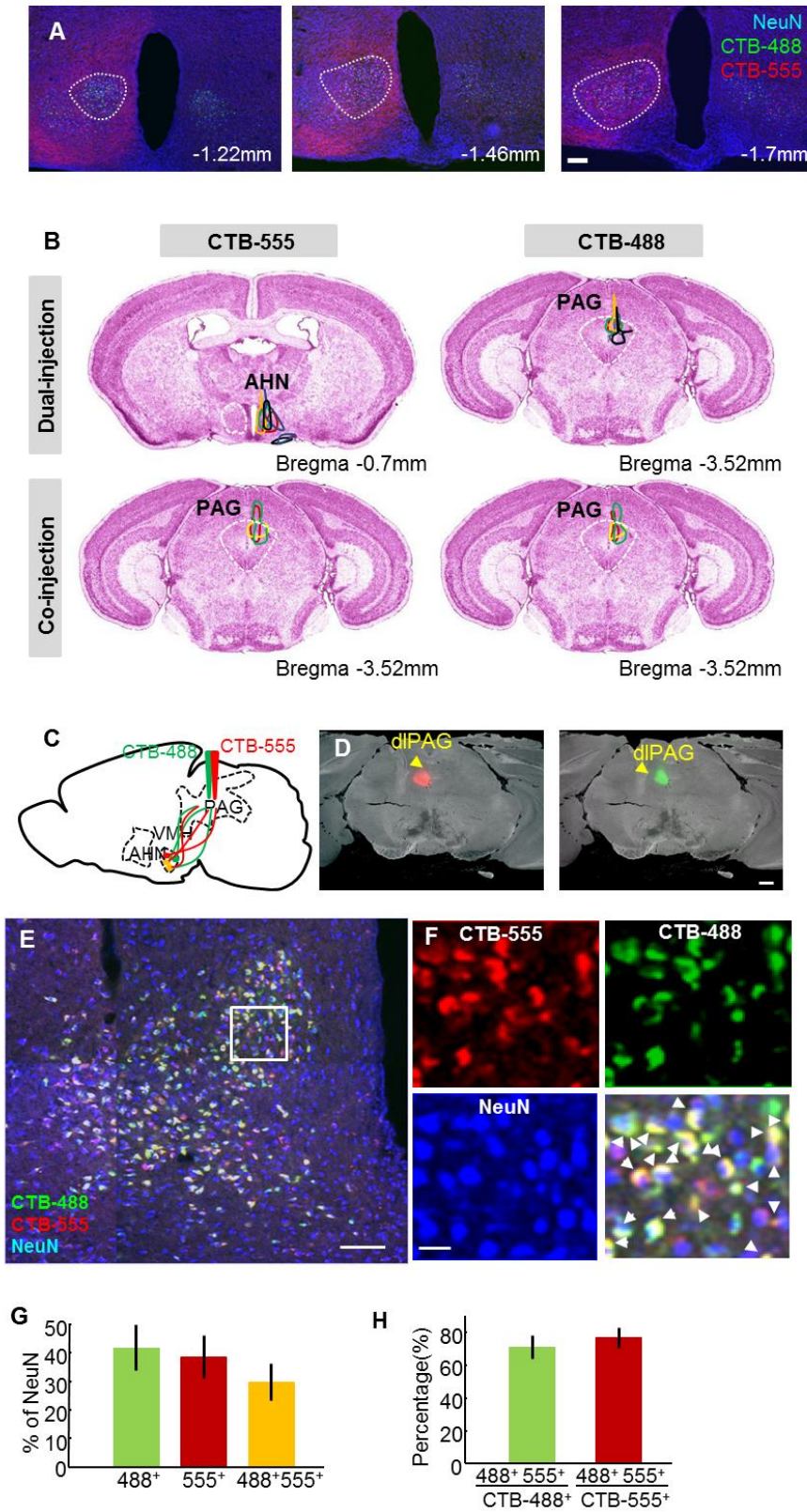
Figure S5 (related to Figure 6). Retrograde labeling to reveal VMH→AHN and VMH→PAG projecting cells. (A) Representative coronal sections at the level of the anterior VMH (Left, Bregma level: −1.22 mm), middle VMH (middle, Bregma level: −1.46 mm) and posterior VMH (right, Bregma level: −1.70 mm). Dashed lines mark the areas used for cell counting. Scale bar: 100 µm. (B) Diagrams illustrate the extent of spread of CTB tracers in AHN and PAG dual-injection (top panels) and PAG co-injection groups (bottom panels). (C) Schematic representation of retrograde tracers co-injected into the PAG. (D) Representative histological pictures showing CTB-555 (left) and CTB-488 (right) injected into dlPAG. Scale bar: 500 µm. (E) VMH neurons labeled with CTB-488 (green) and CTB-555 (red). Blue: NeuN. Scale bar: 100 µm. (F) Individual channels and merged view of the box area in (E). Scale bar: 20 µm. White arrows indicate triple-labeled cells. (G) Percentage of CTB-488 labeled (green), CTB-555 labeled (red) or double-labeled (yellow) neurons among all VMHdm/c neurons. (H) Percentage of double-labeled neurons in CTB-488 or CTB-555 positive population. N = 3 animals. Error bars: standard errors.
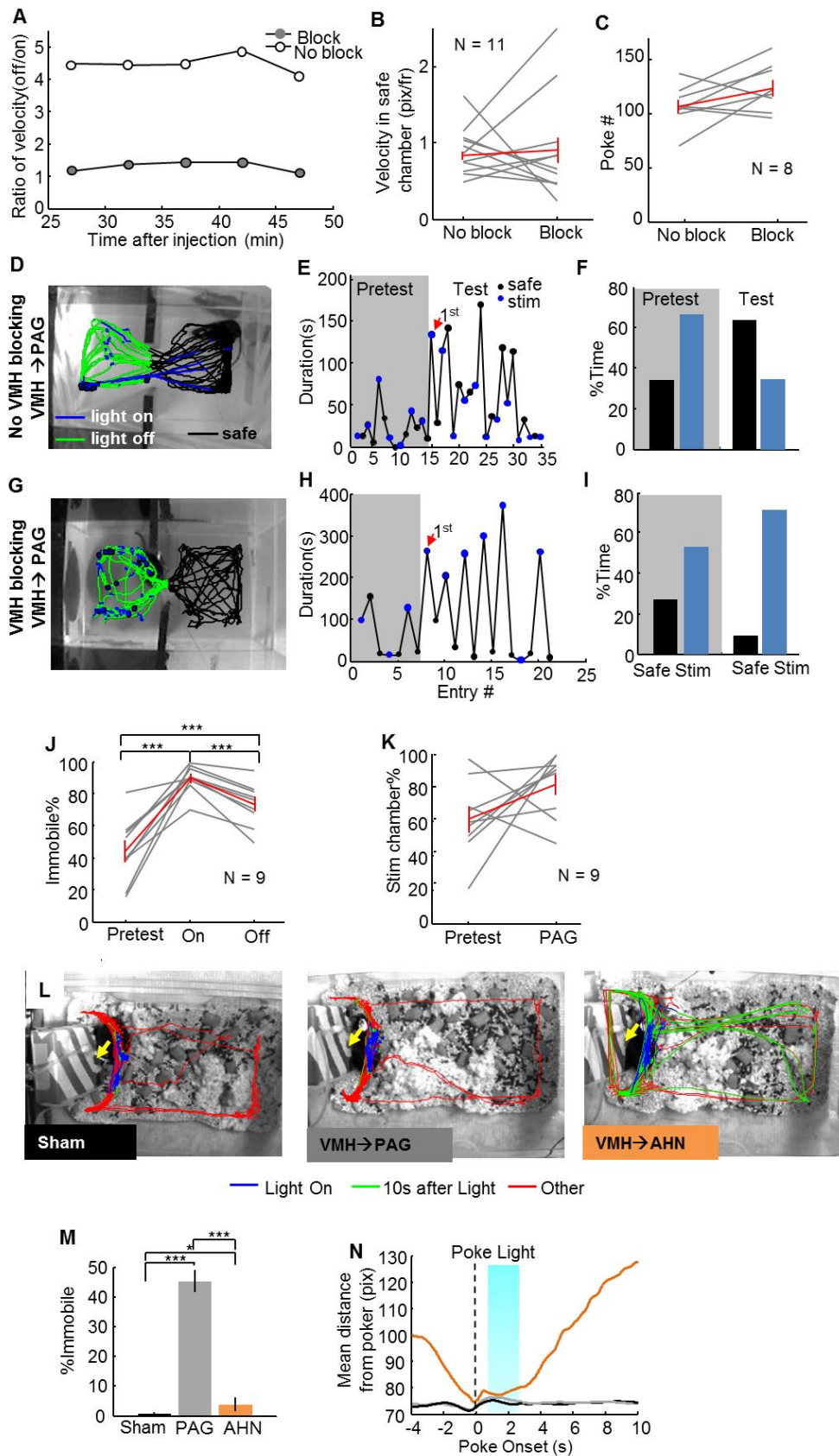
A

B N = 11

C N = 8

D No VMH blocking VMH→PAG
light on
light off — safe

E Pretest Test • safe • stim
1st

F Pretest Test

G VMH blocking VMH→PAG

H 1st
Entry #

I Safe Stim Safe Stim

J *** *** *** N = 9

K N = 9

L Sham VMH→PAG VMH→AHN
— Light On — 10s after Light — Other

M *** *** Sham PAG AHN

N Poke Light
Poke Onset (s)

Figure S6 (related to Figure 7). VMH→AHN and VMH→PAG stimulation induces distinct behavioral changes after VMH blocking. (A) An example plot showing the ratio of velocity during the light-off and light-on periods, with (gray dots) or without (white dots) injection of the VMH with bupivacaine. Bupivacaine eliminates post-stimulation velocity increase and lasts for at least 45 min. (B) The velocity in the safe chamber during the test is not affected by bupivacaine injection (N =11). (C) Poke number during punishment operant conditioning is not affected by bupivacaine injection (N =8). (D–F) An example session of RTPP test with VMH→PAG stimulation without VMH blocking. (G–I) The performance of the same animal as shown in (D–F) with VMH blocking. (D, G) Tracking trace; (E, H) Duration in each chamber over trials; (F, I) Accumulated time in safe (black) and stimulation (blue) chamber during pretest and test. (J–K) During VMH→PAG simulation with VMH blocking, all animals increased immobility (J) and showed no avoidance to the stimulation chamber (K). $***p < 0.001$. N = 9 including 5 animals with confirmed success of VMH blocking and 4 animals with putative VMH blocking based on histology. Gray and red lines indicate data of individuals and population average. (L) Representative tracking traces during the nose poking test during sham, VMH→ANH and VMH→PAG stimulations, all with VMH inactivation. Blue: trace during light on period; green: trace 0–10 s after light; red: other period. Yellow arrows indicate nose ports. Note increased movement towards the corner far away from the poker after VMH→AHN stimulation but not VMH→PAG stimulation. (M, N) In the same session as in (L), VMH→PAG simulation induced higher immobility (M) whereas VMH→AHN simulation caused animal to move away from the nose port (N). Orange: VMH→AHN; black: VMH→PAG; gray: sham stimulation. Error bars: standard errors.
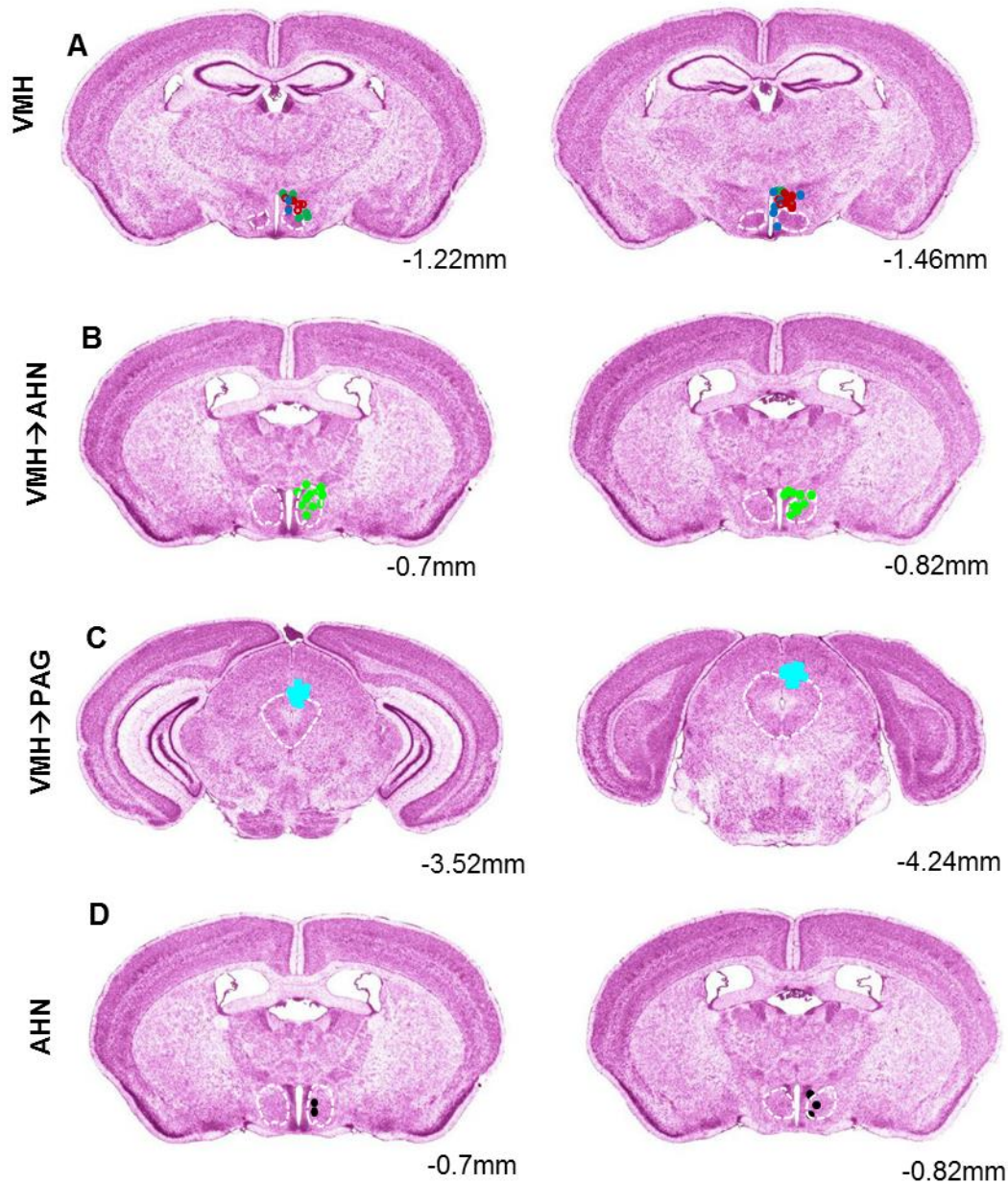
Figure S7 (related to Figure 7). Summary of optic fiber ending positions. (A) Optic fiber ending positions in VMH (N = 29). Red dots: effective blocking of the VMH by bupivacaine injection; blue dots: ineffective blocking of the VMH by bupivacaine injection; red circle: effect of bupivacaine on the VMH was not tested; green dots: other animals. (B) Optic fiber ending

positions in the AHN in VMH→AHN stimulation experiment (green dots, N =24, top panel). (C)

Optic fiber ending positions in the PAG in VMH→PAG stimulation experiment (N = 26).

Histological data from two of the SF1 animals is not available due to technical reasons. (D)

Optic fiber ending positions in the AHN (black dots) in the AHN direct-stimulation experiment
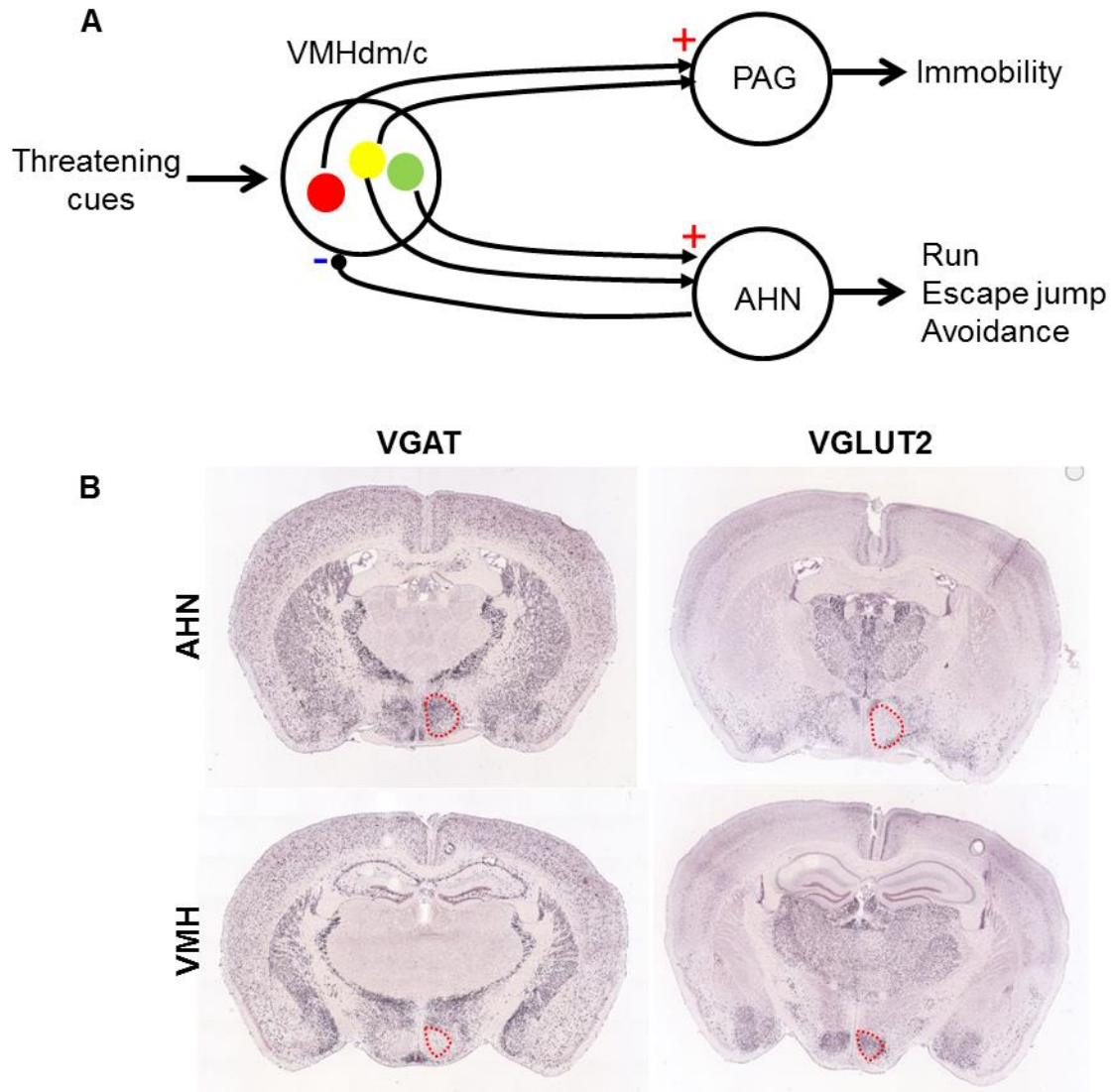
(N = 5).

Figure S8 (related to figure 8) A model of the hypothalamic defense circuit. (A) Threatening signals activate the VMHdm/c which mediates immediate immobility through its direct excitatory projection to the PAG. Simultaneously, an excitatory projection from the VMHdm/c to the AHN mediates flexible escaping response. Upon activation, the AHN may provide negative feedback to the VMHdm/c. (B) In situ hybridization patterns of vesicular GABA transporter (VGAT) and vesicular glutamate transporter 2 (VGLUT2) at the AHN and VMH reveal that whereas VMH cells are mainly glutamatergic, AHN cells are mainly GABAergic.

Dashed lines mark the AHN and VMHdm/c. Images adopted from www.brain-map.org, experiment ID 72081554 and 73818754.

SUPPLEMENTAL TABLE

PAG and AHN dual injection group							PAG co-injection group				
Animal ID \ Cell type	A1	A2	A3	A4	A5	Sum	Animal ID \ Cell Type	B1	B2	B3	Sum
NeuN	1463	1337	539	1269	707	5315	NeuN	690	1594	639	2923
SF1$^+$	1272	1129	434	N/A	N/A	2835	PAG projection CTB-488$^+$	227	864	246	1337
PAG$^+$	790	490	84	568	546	2478	PAG projection CTB-555$^+$	270	785	180	1235
AHN$^+$	778	465	334	530	431	2538	CTB-488$^+$CTB-555$^+$	181	637	148	966
PAG$^+$AHN$^+$	361	133	42	345	292	1173					
PAG$^+$SF1$^+$	594	339	52	N/A	N/A	985					
AHN$^+$SF1$^+$	580	362	197	N/A	N/A	1139					
PAG$^+$AHN$^+$SF1$^+$	299	97	29	N/A	N/A	425					

Animal ID \ Dividing Type	A1	A2	A3	A4	A5	Mean	Animal ID \ Dividing Type	B1	B2	B3	Mean
PAG$^+$/NeuN	54.0	36.6	15.6	44.8	77.2	45.6	CTB-488$^+$/NeuN	32.9	54.2	38.5	41.9
AHN$^+$/NeuN	53.2	34.8	62.0	41.8	61.0	50.5	CTB-555$^+$/NeuN	39.1	49.2	28.2	38.8
PAG$^+$AHN$^+$/NeuN	24.7	9.9	7.8	27.2	41.3	22.2	CTB-488$^+$CTB-555$^+$/NeuN	26.2	40.0	23.2	29.8
PAG$^+$SF1$^+$/PAG$^+$	75.2	69.2	61.9	N/A	N/A	68.8	CTB-488$^+$CTB-555$^+$/CTB-488$^+$	79.7	73.7	60.2	71.2
AHN$^+$SF1$^+$/AHN$^+$	74.6	77.8	59.0	N/A	N/A	70.5	CTB-488$^+$CTB-555$^+$/CTB-555$^+$	67.0	81.1	82.2	76.8
PAG$^+$AHN$^+$SF1$^+$/PAG$^+$AHN$^+$	82.8	72.9	69.0	N/A	N/A	74.9					
PAG$^+$AHN$^+$/PAG$^+$	45.7	27.1	50.0	60.7	53.5	47.4					
PAG$^+$AHN$^+$/AHN$^+$	46.4	28.6	12.6	65.1	67.7	44.1					

Table S1 (related to Figure 6): Summary of retrograde labeling results from PAG and AHN dual injection group (left) and PAG co-injection group (right). The left side of the table shows the total number and percentage of SF1 positive cells and retrogradely labeled cells in the VMHdm/c from individual animals (A1–A5) that were successfully injected with CTB-555 into the AHN and CTB-488 into the dlPAG. The right side of the table shows the total number and percentage of retrogradely labeled cells in the VMHdm/c of individual animals (B1–B3) that were successfully injected with both CTB-488 and CTB-555 into the dlPAG.

SUPPLEMENTAL MOVIE LEGENDS

Movie S1 (Related to Figure 2): Light activation of VMH SF1 neurons induced defensive-like behavior in home cage. The behavioral changes of an animal in its home cage during light stimulation (20 Hz, 20 ms, 2.03 mW) of VMHdm/c SF1 neurons. Animals decreased movement first, then ran around the cage and eventually jumped repeatedly. LED light indicates the light-on period. The movie is played at twice the normal speed.

Movie S2 (Related to Figure 2) Activation of VMH SF1 neurons induced hiding.

In the open arena with a hiding box, the test mouse was stimulated with either real light (20 Hz, 20 ms,1.3 mW) or with sham light (20 Hz, 20 ms, 0 mW) delivered to the VMH for 60 s. Both stimulations started when the animal visited the corner far from the hiding box. During the real stimulation, the mouse quickly ran back to the hiding box and stayed inside for the remaining stimulation period, whereas during the sham trial, the animal continued to eat and to explore the arena. In the absence of a hiding box, with the same VMH stimulation condition, the mouse moved around the arena and eventually stayed immobile in one corner. The movie is played at twice the normal speed.

Movie S3 (Related to Figure 3) Light activation of VMH SF1 neurons induced pupil dilation. The animal was stimulated at the VMH with low intensity (20 Hz, 20 ms, 1 mW) and high intensity (20 Hz, 20 ms, 3 mW) light pulses (20 s each). Both stimulation conditions induced pupil dilation. The movie is played at twice the normal speed.

Movie S4 (Related to Figure 4): Light activation of VMH SF1 neurons induced avoidance to the stimulation chamber in a real-time place preference test. During the first entry into the stimulation chamber, the animal increased immobility during light stimulation (20 Hz, 20 ms, 2.85 mW, 3 s light-on interleaved with 2 s light-off) and stayed in the chamber for more than 200 seconds. By the forth trial, the mobility of the animal decreased during light stimulation. Instead, it quickly moved back into the safe chamber. LED indicates the light-on period. The movie is played at twice the normal speed.

Movie S5 (Related to Figure 5): Light stimulation of VMH→ PAG and VMH → AHN induced behavioral changes in home cage. Whereas VMH→ PAG stimulation (20 Hz, 20 ms, 4.08 mW) induced only immobility, VMH→AHN stimulation (20 Hz, 20 ms, 1.49 mW) induced immobility, running and jumping in the same animal. LED indicates the light on period. The movie is played at twice the normal speed.

Movie S6 (Related to Figure 8): Light stimulation of the AHN induced running and escape jumping but no immobility. The ventral AHN of a wild-type C57BL/6 animal was injected with AAV2 that expressed both CRE and CRE-dependent ChR2. Three weeks later, the animal was stimulated at the AHN (20 Hz, 20 ms, 2.3 mw) for 1 min in its home cage. Stimulation induced running, repeated wall rearing and jumping. LED indicates the light-on period. The movie is played at twice the normal speed.

Movie S7 (Related to Figure 8): Light activation of AHN neurons induced avoidance to the stimulated chamber in a real-time place preference test.

The ventral AHN of a wild-type C57BL/6 animal was injected with AAV2 expressing both CRE and CRE dependent ChR2. During the pretest, the animal showed a slight preference for the left chamber. During the test, the animal was stimulated at the AHN (20 Hz, 20 ms, 3.3 mW, 3 s light-on interleaved with 2 s light-off) whenever it entered the left chamber. Upon stimulation, the animal showed no immobility and quickly moved out of the stimulation chamber. Also, the animal spent longer time in the safe chamber before it re-entered the stimulation chamber. The movie is played at twice the normal speed.

EXTENDED EXPERIMENTAL PROCEDURES

Animals

SF1-CRE transgenic mice were provided by Dr. Lowell group at Harvard University and are currently available from Jackson laboratory (stock No. 012462) (Dhillon et al., 2006). A breeding colony was maintained by mating SF1-CRE mice with C57BL/6N mice (Charles River) at New York University Langone Medical Center (NYULMC). Adult male and female SF1-CRE mice (8–24 weeks) were used for all behavioral and electrophysiological experiments targeting the VMH; wild-type littermates were used for tracing studies. Adult wild-type C57BL/6N male and female animals (10-16 weeks, Charles River) were used for AHN manipulation. To reveal the CRE expression pattern, SF1-CRE mice were mated with GFP reporter mice (RCE:loxP line, provided by Dr. Fishell lab at NYULMC) (Sousa et al., 2009). Mice were maintained on a reversed 12-hour light/dark cycle (noon to midnight as dark cycle) and given food and water *ad libitum*. All experiments were performed between noon and 7 pm. All procedures were approved by the IACUC of NYULMC in compliance with the NIH guidelines for the care and use of laboratory animals.

Stereotactic surgery and injection

To target the VMH, each animal was injected unilaterally with 0.32 μl AAV2/2 (4.9×10^{13} PFU/ml, UNC Vector Core) coding for Cre dependent ChR2-EYFP under the control of the EF1α promoter (coordinates: –4.5 mm AP, +0.4 mm ML, –5.4 mm DV). To target the ventral AHN, 0.18 μl 1:2 mixed AAV2/2 CMV:CRE (1.9×10^{14} PFU/ml, University of Iowa) and

AAV2/2 ER1α:DIO-ChR2-EYFP (4.2×10^{13} PFU/ml , UNC Vector Core) was injected (coordinates: –4.5 mm AP, +0.4 mm ML, –5.4 mm DV). Injection was done using a Nanoliter injector (World Precision Instruments) at a speed of 20 nl/min, followed by an additional 10 min before retraction (Chan et al., 2007). For optogenetic stimulation, a double cannula (5.4 mm, 26 G thin wall stainless steel tubing, center to center distance is 1.0 mm, Plastics One) was implanted 0.4–0.8 mm above the VMHdm/c (–4.5 mm AP, 0.4 mm ML, –4.6 mm DV) and AHN (–3.5 mm AP, +0.4 mm ML, –4.6 mm DV), and in some cases a 230-μm multimode optic fiber (Thorlabs) with 1.25-mm ferrule was implanted 0.5 mm above dlPAG (–7.7 mm AP, 0.2 mm ML, –1.9 mm DV). All implanted components were secured to the skull with dental cement (Metabond, Parkell).

For *in vivo* recording, we modified our chronic *in vivo* recording electrode to include sixteen 13-μm tungsten microwires and one 105-μm multimode optic fiber (Thorlabs) (Lin et al., 2011). The tip of the optic fiber was etched by dipping into hydrofluoric acid for 10 min (Stark et al., 2012). The optrode was attached to a moveable microdriver and inserted above the putative VMHdm/c (initial implantation position: –4.5 mm AP, +0.35 mm ML, –5.0 mm DV) after virus injection, and secured with bone screws and dental cement.

For tracing, 0.12 μl of 1 mg/ml CTB-555 in PBS (Life Technologies) was injected into the AHN (–3.5 mm AP, +0.35 mm ML, –5.0 mm DV) and 0.12 μl of 1 mg/ml CTB-488 was injected into the dlPAG (–7.7 mm AP, +0.2 mm ML, –2.4 mm DV) of the same animal at a speed of 20 nl/min. After injection, the glass capillary was left in place for 20 min to allow diffusion. For control, both CTB-555 and CTB-488 were injected into the dlPAG at the same coordinates (–7.7 mm AP, +0.2 mm ML, –2.4 mm DV) but with two penetrations. Animals were perfused one week after injection to harvest brains for histological analysis.

For VMHdm/c blocking, 0.3 µl TTX (1 µM, Tocris or R&D Systems), 8% lidocaine (Sigma) or 4% bupivacaine (Sigma) dissolved in 0.9% saline were used. Under light anesthesia, drug was administered into the brain using a 0.5-µl Neuros syringe (Hamilton) mounted on a vertical syringe pump (World Precision Instruments). The beveled 31 G syringe needle was lowered through the guide cannula to 5.4 mm, and 0.15 µl of drug was injected at 0.9 nl/s. The injection was repeated after retracting the needle to −5.3 mm, and followed by 2-min wait before full retraction. Behavioral tests started 15 min after the final injection.

Optrode recording and analysis

Two weeks after injection, we connected the implanted optrode with a sixteen-channel headstage and a 105-µm multimode optic fiber. Neural activity and light stimulation was then recorded from the freely moving animal (Tucker-Davis Technologies) and band-pass filtered between 100 and 5,000 Hz. Blue light pulses (1 ms, 5 Hz) were delivered to activate cells. The final light intensity at the tip of the optrode was between 0.17 to 0.27 mW. Direct activation of a ChR2-expressing cell was determined if (1) the cell can follow a 1-ms light activation with a latency <5 ms and jitter < 1 ms, as suggested by previous recording from other brain regions (Jennings et al., 2013); (2) the light-evoked spike waveform is similar to the spontaneous spike waveform. Spike sorting was performed using OfflineSorter (Plexon Instruments). The placement of the optrode was examined histologically. After the first recording, the implanted optrode was slowly moved down in 70-µm increments until it reached 5.6 mm. The peristimulus histogram (PSTH) for light stimulation was generated by averaging the firing rate of a recorded cell aligned to the light onset.

Behavioral tests

The behavioral tests were done between 2 to 8 weeks after surgery. To deliver light to the VMH and/or AHN, two 230-μm multimode optic fibers were inserted into the cannulas and secured with a matching cap (Plastics One). To deliver light to the PAG, a 230-μm multimode optic fiber with ferrule was connected to the implanted optic fiber ferrule assembly with a matching sleeve. The light transmission efficiency between the ferrule and the implanted optic fiber was above 70%. The other end of the optic fiber was connected to a 100-mW 473 nm blue laser (Shanghai Dream Lasers) controlled by computer programmed TTL pulses.

In the home cage test, for VMH and AHN stimulation, blue light (20 Hz, 20 ms) with a range of intensities (1–6 mW) and frequencies (5, 10, 15 and 20 Hz) was randomized and delivered for at least 5 times per condition. For PAG stimulation, animals were stimulated with 20 Hz, 20 ms, 3–6 mW light. For VMH and its terminal stimulations, each trial lasted for 60 s unless we observed jumping, which would terminate the trial. For direct stimulation of the AHN, each trial lasted 60 s regardless of the behavioral response. Running was defined as fast movement typically along the edges of the cage. Jumping was defined as vertical movement with all paws leaving the ground. One to two minutes were allowed between adjacent stimulations. To test the effect of brief stimulation on locomotion, 2 s, 20 Hz, 20 ms stimulation (1–2 mW) was delivered every 30 s for 30 min. To examine light-induced Fos expression, animals were stimulated with 20 s, 20 Hz, 20 ms light at 2–4 mW for 20 times in the home cage and perfused with 4% paraformaldehyde 1 hour later. For sham stimulation controls, optic fiber was connected but no light was delivered.

For the hiding box test, the animal was placed in an arena (L×W×H = 60×60×30 cm) with a cardboard box in one corner (L×W×H = 9×18×20 cm with closed top). Five to ten food pellets were scattered on the floor away from the hiding box to encourage continuous exploration. After the animal was habituated to the arena for 10 min, interleaved real (1-×.3 mW, 20 ms, 20 Hz, 60 s) and sham stimulation trials (0 mW, 60 s) were initiated whenever the animal reached one designated corner far away from the hiding box. After 6–8 pairs of stimulation trials were completed, the hiding box was removed and the animal was stimulated with the same stimulation protocol for 6 more times.

For the RTPP test, the arena contains two chambers (L×W×H = 13×19×30 cm) connected with a 6-cm wide opening. Each chamber has different contextual cues on the wall. During the test, when four paws of the test animal were in the stimulation chamber, the stimulation was manually initiated. Once triggered, it interleaved between 3-s on and 2-s off until animal exited from the stimulation chamber (all four paws out). The apparatus was cleaned with 70% ethanol thoroughly after each test. For a given animal, if multiple brain sites (VMH, AHN, PAG) were tested with the paradigm, each brain site was tested on separated days.

In the punishment operant conditioning, animals were deprived of water for 19 hours and a nose poking panel (Med Associates) and a TTL pulse triggered water delivery device were inserted into animal's home cage right before the test. When an animal successfully held its nose snout in the poker for more than 50 ms, it dimmed the backlit indicator in the poker for 1s, triggered the water valve to immediately open for 50 ms and turned on light stimulation for 2 s after 0.8 s delay. Water was delivered through a 24-G syringe needle positioned 2 cm away from the poker. In the 1 s period when the indicator light was off, further poking did not trigger

additional water delivery. All stimulation and behavioral events were recorded synchronously (Streampix, Norpix).

Behavioral analysis

We used the paired Student's *t*-test to examine the effect of stimulation on several parameters of home cage behavior: (1) the percentage of time each animal spent immobile during light delivery (light), 30 s before light (before) and 30 s after light (after); (2) the percentage of before, light and after trials during which running or jumping was observed; (3) the mean velocity during accumulated before, light and after periods; and (4) mean latency to immobility, running and jumping under different stimulation conditions. The "low" intensity refers to the minimal intensity required to induce behavioral changes, ranging from 0.8 mW to 3.5 mW. The "high" intensity refers to three times of the minimal intensity up to 6 mW. For each animal, we varied stimulation frequency from 5 to 20 Hz in 5 Hz increments. If a clear behavioral change was observed at 5 Hz stimulation, low, medium and high frequency refer to 5, 10 and 15 Hz. Otherwise, they refer to 10, 15 and 20 Hz. Latency to immobility, running or jumping refers to the average time interval from the light onset to the behavior onset across stimulation trials. If no running or jumping was observed at a given frequency for an individual, 60 s was used for calculation. Only trials not annotated as "immobile" at the onset of the trial were used to calculate the latency to immobility.

For the RTPP test analysis, we calculated the following parameters for each animal and used the paired *t*-test to examine the effect of stimulation: (1) the mean duration in the stimulation and safe chambers per entry during the pretest and testing periods; (2) the percentage

of total time spent in the stimulation chamber during the pretest and test periods; (3) the percentage of total time spent immobile during the pretest, stimulation-on and stimulation-off periods.

We examined the effect of light activation on the nose poking test with the paired *t*-test using following parameters: (1) number of successful poking events with real or sham stimulation; (2) the percentage of total time an animal spent immobile during accumulated real or sham stimulation period; (3) the maximum distance to the poker within 10 s after sham or real stimulation averaged across trials. To examine the immobility during stimulation, we manually annotated "immobility" during the 2-s stimulation based on both side and top views. For a frame to be considered "immobile" with manual annotation, the animal has to show no clear movement of any body parts, including limbs, head and tongue. Error bars indicate standard errors in all figures. When the paired *t*-test was performed for parameters involving three groups (e.g., before, light and after), the *p* value was adjusted with a false discovery rate of 0.05.

Recording of pupillary, respiratory and cardiovascular responses and analysis

To monitor the pupillary response, a brass head plate (3.4 mm x 5.5 mm x 2 mm with two threaded holes) was cemented on an animal's skull and a holding rod was attached to the plate using two 00-90 screws during the experiment. The head-fixed animal was placed onto a single axis rotating styrofoam ball (20 cm in diameter) to permit locomotion. An infrared-sensitive camera was used to capture the pupil image under infrared lighting. After acquiring the video, we detected the pupil in each frame using a custom written Matlab script based on the Hough transform circle recognition algorithm. The ratio of the circle diameter during stimulation and

baseline (time matched period prior to each stimulation trial) was calculated to quantify the light induced pupillary response. To determine pupil response during running, we manually annotated the running events and calculated the average PSTH of pupil diameter aligned to running onset using an 80-ms time bin (2 video frames).

Breathing was manually counted based on chest movement using videos recorded from head-fixed animals. Only periods when individual chest movement could be clearly discerned were used for analysis. Breathing rate was calculated as the accumulated number of breathings divided by the accumulated stimulation or baseline period. Baseline is the time-matched period prior to each stimulation trial. The ratio between breathing rate during stimulation period and baseline was then calculated as the response during light.

To monitor the cardiovascular response in freely moving animal, we placed three insulated multi-stranded stainless steel wire leads (A-M system, NO. 793200) subcutaneously under general anesthesia (Ho et al., 2011). Briefly, the three wires were connected to an omnetics connector cemented onto the mouse back and tunneled underneath the skin to reach each of three recording positions (left arm, right arm and right leg). Each tip of the wire was made bare by removing 3 mm insulation from the wire to create the contact surface. The end of the wire was brought out from a small skin incision and multiple knots were tied to prevent the wire from retraction. During recording, the ECG signal passed through a commutator and collected using a commercial recording system (Tucker-Davis Technologies) at 3000 Hz. Then, the raw ECG signal was band-pass filtered (10–1000 Hz) and a custom written Matlab program was used to detect the peaks of the ECG trace (Figure 3E, red dots). The instantaneous HR was calculated as the inverse of the inter-beat-interval. The HRV for a given period was calculated as standard deviation of HR/mean of HR. To determine light induced HR response in each animal, we

calculated the average HR and HRV during light-on, –30 to 0 s before light and 0–30 s after light for each stimulation trial. Then, we used the paired *t*-test to determine any significant changes in HR and HRV during the light-on period compared with the before- or after-light period. To determine the HR change during running, we used our computer-based auto-annotation program to determine all the running events and calculated the PSTHs of HR aligned to running onset using 100-ms time bins.

Histology and immediate early gene expression analysis

Standard immunohistochemistry procedures were followed to obtain and stain the 30-µm brain sections for all mice. Rabbit anti-SF1 (1:100, TransGenic), goat anti-Fos (1:300, Santa Cruz Biotechnology), mouse anti-NeuN (1:300, Millipore), rabbit anti-GFP (1:300, Life Technologies), donkey anti-mouse Dylight 405 (1:300), donkey anti-rabbit Dylight 488 (1:300, Jackson Immunoresearch) and donkey anti-goat Dylight 555 antibodies (1:300, Jackson Immunoresearch) and DAPI (1:20,000, Life Technologies) were used. For determination of cannula, optic fiber and optrode placements and tracer injection sites, 2.5× or 5× fluorescent images were acquired. For Fos cell counting, 10× fluorescent images were used. For tracing studies, 20× confocal images were obtained.

To count cells, we first selected regions of interest based on counterstaining and then manually counted cells in the red and/or green channels by using a custom-written Matlab program. To quantify YFP distribution in the VMHdm/c vs. VMHvl, the ratio of the accumulated pixel values in the green channel in the VMHdm/c and VMHvl was calculated for

each section and then averaged across sections for each animal. The Student's *t*-test was used to determine whether the ratio is significantly different from 1 across the animals.

To compare the Fos expression under various stimulation condition, two-way ANOVA was used for each stimulation condition to reveal the main factors contributing to the Fos number variability (stimulation side vs. non stimulation, real stimulation vs. sham stimulation and their interaction term), followed by the paired *t*-test.

Tracking and annotation comparison

Custom tracking software written in MATLAB was used to determine the instantaneous position of the recorded mouse based on side- and top-view videos (Burgos-Artizzu et al., 2012; Dollar et al., 2010). The instantaneous XY and Z velocities of each frame were calculated as the difference in center location of the animal in current and previous frame. We defined "immobility" as when the animal moves for less than 0.5 pixel/frame at the XY plane and the movement lasts for at least 2 s. "Running" was defined as when locomotion is above 8 pixel/frame with a maximum speed above 20 pixel/frame and lasts for minimally 0.2 s. "Jumping" was defined as events that lead to the animal's center location elevated for at least 120 pixels above the ground and with maximum vertical movement speed above 20 pixel/frame. In our video, each pixel represents approximately 0.5 mm and the videos were taken at 25 frame/sec. A total of 269 hours of videos were analyzed to determine the behaviors using these parameters.

To evaluate the performance of computer annotation, 3.8 hours of behavioral videos were annotated manually by two experienced human annotators frame by frame (sample period shown

in Figure S2C). Then, we compared the computer and human annotated immobility, running and jumping events during the 79 light-stimulation trials (approximately 60 s per trial). We found that consistency between the human-computer annotations is comparable to the human-human annotations. For immobility, we calculated the percentage of time animal spent immobile for each light stimulation period and found that the Pearson correlation coefficient (r) between two human annotators is 0.827, whereas the correlation coefficients of computer and two human annotators are 0.781 and 0.802, respectively (Figure S2D). For running, we calculated the number of running events during each light stimulation period and found correlation coefficient of human-human annotation is 0.864 whereas correlation coefficients of human-computer annotation are 0.850 and 0.944 (Figure S2E). For jumping, we calculated the number of jumps within 30 s after the light stimulation, given that most jumping events occurred after light stimulation instead of during light stimulation in these three randomly selected videos (Figure S2C). The correlation coefficient for human annotators is high ($r = 0.9611$), given that jumping events are distinct and hard to miss. Although the computer missed about 20% of jumping events, its overall performance still correlated well with human performance ($r = 0.9093$ and 0.9192) (Figure S2F). Thus, we determined that the performance of the automated annotation program is sufficiently reliable to identify the behaviors of interest.

SUPPLEMENTAL REFERENCES

Burgos-Artizzu, X.P., Dollár, P., Lin, D., Anderson, D.J., and Perona, P. (2012). Social Behavior Recognition in continuous videos. Paper presented at: IEEE Conference on Computer Vision and Pattern Recognition (Providence, Rhode Island).

Chan, E., Kovacevic, N., Ho, S.K., Henkelman, R.M., and Henderson, J.T. (2007). Development of a high resolution three-dimensional surgical atlas of the murine head for strains 129S1/SvImJ and C57Bl/6J using magnetic resonance imaging and micro-computed tomography. Neuroscience *144*, 604-615.

Dhillon, H., Zigman, J.M., Ye, C., Lee, C.E., McGovern, R.A., Tang, V., Kenny, C.D., Christiansen, L.M., White, R.D., Edelstein, E.A.*, et al.* (2006). Leptin directly activates SF1 neurons in the VMH, and this action by leptin is required for normal body-weight homeostasis. Neuron *49*, 191-203.

Dollar, P., Welinder, P., and Perona, P. (2010). Cascaded Pose Regression. Paper presented at: IEEE Conference on Computer Vision and Pattern Recognition

Ho, D., Zhao, X., Gao, S., Hong, C., Vatner, D.E., and Vatner, S.F. (2011). Heart Rate and Electrocardiography Monitoring in Mice. Current protocols in mouse biology *1*, 123-139.

Jennings, J.H., Sparta, D.R., Stamatakis, A.M., Ung, R.L., Pleil, K.E., Kash, T.L., and Stuber, G.D. (2013). Distinct extended amygdala circuits for divergent motivational states. Nature *496*, 224-228.

Lin, D., Boyle, M.P., Dollar, P., Lee, H., Lein, E.S., Perona, P., and Anderson, D.J. (2011). Functional identification of an aggression locus in the mouse hypothalamus. Nature *470*, 221-226.

Sousa, V.H., Miyoshi, G., Hjerling-Leffler, J., Karayannis, T., and Fishell, G. (2009). Characterization of Nkx6-2-derived neocortical interneuron lineages. Cereb Cortex *19 Suppl 1*, i1-10.

Stark, E., Koos, T., and Buzsaki, G. (2012). Diode probes for spatiotemporal optical control of multiple neurons in freely moving animals. Journal of Neurophysiology *108*, 349-363.